

Quantitative stiffness of the median nerve, flexor tendons, and flexor retinaculum in the carpal tunnel measured with acoustic radiation force impulse elastography in various wrist and finger positions

Sungche Lee, MD^a, Jinmyong Kwak, MD^a, Sanghoon Lee, MD^a, Hyuncheol Cho, MD^a, Eunsun Oh, MD^b, Ji Woong Park, MD, PhD^{a,*}

Abstract

Despite the high prevalence and clinical importance of soft-tissue disorders, objective methods for evaluation of the biomechanical properties of soft tissues are lacking. This study aimed to quantitatively evaluate stiffness, an important biomechanical characteristic of soft tissue, using acoustic radiation force impulse (ARFI) elastography. The shear wave velocity (SWV, m/s) values of soft tissue structures within the carpal tunnel (CT) were measured in various combinations of wrist and finger positions.

Twenty-six healthy adults were enrolled in this study. We measured the cross-sectional area of the median nerve (MN) and the SWV values of several structures within the CT at the CT inlet level. Measurement of SWV of the MN, flexor digitorum superficialis (FDS), flexor digitorum profundus (FDP), and transverse carpal ligament (TCL) were conducted in six wrist/finger motion combinations.

When the wrist and fingers were in neutral positions (position A), the mean SWV was lowest for the MN (mean \pm standard deviation, 2.3 ± 0.5 m/s), followed by the FDS (2.9 ± 0.2), FDP (3.2 ± 0.3), and TCL (3.3 ± 0.4). The SWV was significantly different among the six different wrist/finger positions for all structures ($P < .001$). However, the MN cross-sectional area was not significantly different ($P = .527$). The SWV values for the MN, FDS, and FDP increased significantly as the wrist/finger positions the stress on the tendons increased (from position B to F) compared with a neutral position, while the SWV of the TCL was significantly higher for in all positions compared with neutral, except for wrist neutral, finger extension. The SWV values for the MN, FDS, and TCL gradually increased as stress increased.

The intra-CT structures are under increased stress during wrist and finger motions than when the hand is in a neutral position. We have used ARFI elastography to gain insight into the pathophysiology of CTS.

Abbreviations: ARFI = acoustic radiation force impulse, CTS = carpal tunnel syndrome, FDP = flexor digitorum profundus, FDS = flexor digitorum superficialis, ICC = intraclass correlation coefficient, MN = median nerve, MN CSA = median nerve cross-sectional area, SWV = shear wave velocity, TCL = transverse carpal ligament.

Keywords: carpal tunnel, elastography, median nerve, stiffness

Editor: Neeraj Lalwani.

This research was supported by the Soonchunhyang University Research Fund.

The Institutional Review Board approval number: SCHUH 2017-05-007-001

The South Korea Clinical Trials Registry number (at <https://cris.nih.go.kr>): KCT0002464

The authors report no conflicts of interest.

^a Department of Physical Medicine and Rehabilitation, ^b Department of Radiology, Soonchunhyang University Seoul Hospital, Soonchunhyang University College of Medicine, Seoul, Republic of Korea.

* Correspondence: Ji Woong Park, Department of Physical Medicine and Rehabilitation, Soonchunhyang University Seoul Hospital, Soonchunhyang University College of Medicine, 59 Daesagwan-ro, Yongsan-gu, Seoul 04401, Republic of Korea (e-mail: spotdoc@schmc.ac.kr).

Copyright © 2019 the Author(s). Published by Wolters Kluwer Health, Inc. This is an open access article distributed under the terms of the Creative Commons Attribution-Non Commercial-No Derivatives License 4.0 (CCBY-NC-ND), where it is permissible to download and share the work provided it is properly cited. The work cannot be changed in any way or used commercially without permission from the journal.

How to cite this article: Lee S, Kwak J, Lee S, Cho H, Oh E, Park JW. Quantitative stiffness of the median nerve, flexor tendons, and flexor retinaculum in the carpal tunnel measured with acoustic radiation force impulse elastography in various wrist and finger positions. *Medicine* 2019;98:36(e17066).

Received: 29 January 2019 / Received in final form: 8 June 2019 / Accepted: 12 August 2019

<http://dx.doi.org/10.1097/MD.0000000000017066>

1. Introduction

Carpal tunnel syndrome (CTS) accounts for 90% of all neuropathies and can cause impaired fine motor function, work performance hindrance, and financial loss.^[1,2] The condition presents as varied symptoms, singly or in combination, with patients typically reporting tingling, numbness, and pain in the median nerve (MN) territory.^[3,4]

Damage to the MN is caused by pressure and localized ischemia due to external pressure,^[4] either direct pressure from the surrounding tissues or pressure due increased interstitial fluid pressure within the CT.^[5] During hand movements, motions of the tendons cause stretching, compression, and/or shearing force of the structures within the CT, compressing the surrounding structures. Blockage of venous outflow by such forces causes nerve inflammation and edema in the entrapment area. This increases the interstitial fluid pressure, further increasing the pressure in the CT and causing ischemia, resulting in a cycle of cell damage due to ischemia and tissue edema.^[3-5] Increasing our understanding of the mechanics of the structures in the distal upper limb is essential in order to understand and treat wrist-entrapment neuropathy.^[3,6,7]

All these mechanisms make understanding and diagnosing CTS difficult. Currently, clinical examination is vital for

diagnosis; electrodiagnostic testing is the gold standard as it enables determination of the severity of CTS and detection of early changes.^[4,8] Ultrasound examination enables real-time static and dynamic analyses of anatomical structures, and B-mode ultrasound enables direct assessment of the size and shape of the MN cross-section within the CT and the pathology of the surrounding structures. However, B-mode analysis of the morphology of the MN alone is not enough to confirm the severity or pathophysiology of CTS.^[1,9–11]

Acoustic radiation force impulse (ARFI) elastography is a popular ultrasound technique, and ARFI elastography provides a quantitative measurement of stiffness by calculating the shear wave velocity (SWV). Previous studies have shown that the stiffness of the MN is higher in CTS patients compared with healthy people, and that ARFI elastography can be used to determine the severity of CTS.^[1,3,9] However, to the best of our knowledge, no reports have measured the stiffness of structures within the CT in healthy individuals to understand normal biomechanics during hand motions.

In this study, we used ARFI elastography to measure the SWV values of the soft-tissue structures within the CT of healthy volunteers in various hand positions. We analyzed the differences in order to gain insight into the pathophysiology of CTS and investigate the clinical efficacy of ARFI elastography.

2. Materials and methods

2.1. Study design

The present study was a cross-sectional study conducted from July 2017 to June 2018 in Soonchunhyang University Hospital (SCHUH), Seoul, South Korea. This study and all of its protocols were approved by the Institutional Review Board of SCHUH (SCHUH 2017–05–007–001) and was registered in the South Korea Clinical Trials Registry at <https://cris.nih.go.kr> (KCT0002464). All participants provided written informed consent for publication. There were no changes in the research plan during the study.

2.2. Participants

The present study recruited healthy adults aged 19–65 years. Exclusion criteria were: musculoskeletal disorders or deformation in both hands and wrists (such as amputation, burn, or contracture); presence of focal neuropathies (such as radiculopathy or CTS); MN deformity revealed through ultrasound examination; central nervous system lesions; and/or those who had difficulty with testing due to pain, deformity, or cognitive impairment.

2.3. Acoustic radiation force impulse elastography

Two researchers (both with 4 years of experience in ARFI elastography) examined the participants. Information regarding the method and results of the exam were not shared among the researchers. The 9L4 Linear Array Transducer was used with the ACUSON S2000 system (Siemens Medical Solutions USA Inc., Mountain View, CA) for this study. Participants sat upright after placing the nondominant hand (less-used hand for ambidextrous participants) on the examination table with the elbow joint at 90°. Each participant was asked to perform three finger motions: neutral position (relaxed), grasp, and extension (0° in metacarpophalangeal, proximal interphalangeal, and distal interphalangeal joints) at two wrist angles (0° and 30° extension^[12]). Two custom-made plastic splints were used to secure the wrist joint



Figure 1. Acquiring B-mode and acoustic radiation force impulse images at the carpal tunnel inlet. The wrist and finger positioning for B-mode and acoustic radiation force impulse elastography measuring. The nondominant hand was stabilized with a custom-made plastic splint during measurement in neutral positions and wrist in 30° extension. The transducer was located on the carpal tunnel inlet, transversely.

(Figure 1). The following six finger/wrist motion combinations were performed in one testing session and were measured with ARFI imaging: (A) wrist neutral (0°), finger neutral; (B) wrist neutral, finger grasp; (C) wrist neutral, finger extension; (D) wrist extension (30°), finger neutral; (E) wrist extension, finger grasp; and (F) wrist extension, finger extension. An ultrasound transducer was placed on the CT inlet (pisiform bone to scaphoid tubercle) of the participant and measured in transverse view. Targets of interest were the MN, flexor digitorum superficialis (FDS), flexor digitorum profundus (FDP), and transverse carpal ligament (TCL). One examiner measured the SWV of the structures thrice per motion and the mean value of the three was used for analysis. Another examiner repeated the examination to obtain the intraclass correlation coefficient (ICC).

Next, ARFI elastography measurements were conducted in the following order: first, MN, FDS, FDP, and TCL were confirmed via conventional B-mode imaging in the carpal tunnel inlet level (Figure 2A). For qualification of ARFI images, we confirmed that the green color map was uniform in the qualification mode (Figure 2B). Next, an SWV color map was overlaid on the B-mode image to obtain the ARFI elastography image (Figure 2C). In the ARFI image, different colors were used to illustrate the level of stiffness. To quantitatively analyze the SWV of the target structures, seven $2 \times 2 \text{ mm}^2$ regions of interest were marked on each ARFI image color map. Boxes marking these regions of interest were placed on the center of the MN, on the 2nd and 3rd tendons of the FDS and FDP, and on the two points that divide the TCL into three (Figure 2C and D).

The MN cross-sectional area (MN CSA, mm^2) was measured on the B-mode image by drawing a continuous line following the hypochoic inner delineation of the MN in the ultrasound machine, which allowed the software to automatically calculate the CSA.^[11]

2.4. Statistical analysis

To estimate the appropriate number of subjects for this research, we followed the model of a previous research that analyzed the

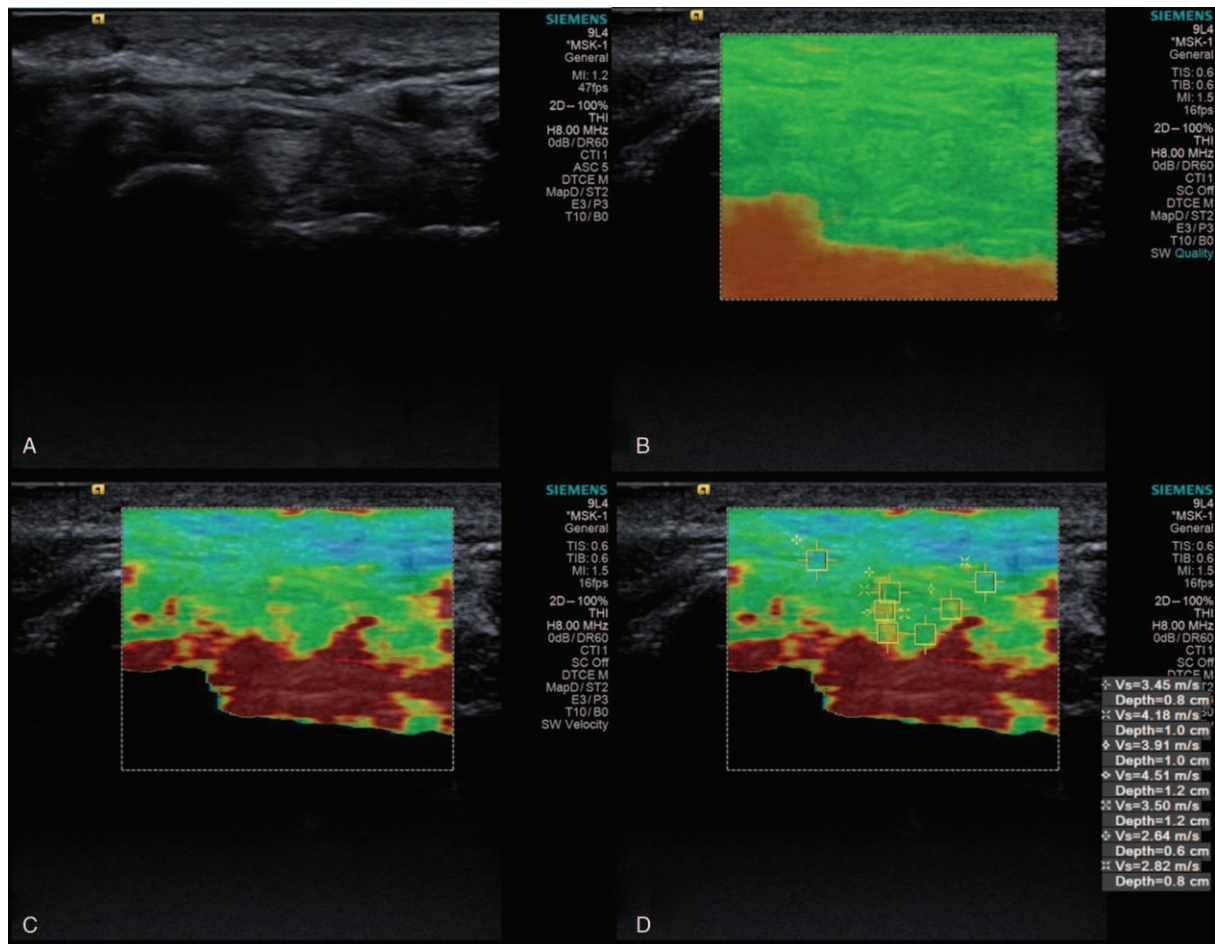


Figure 2. Measuring the shear wave velocity of target structures using acoustic radiation force impulse elastography. (A) Representative B-mode image at the carpal tunnel inlet showing target structures such as the median nerve, flexor digitorum superficialis, flexor digitorum profundus, and transverse carpal ligament. (B) Qualification of the acoustic radiation force impulse image. A homogenous green color map indicates a good-quality image. (C) Acquired acoustic radiation force impulse images and region-of-interest box placement for measuring shear wave velocity. A total of seven boxes were placed on the image (top to bottom of the image): two for the transverse carpal ligament, one for the median nerve, two for the flexor digitorum superficialis, and two for the flexor digitorum profundus. Red, green, and blue hues indicate high, medium, and low stiffness, respectively.

red pixel intensity of the Achilles tendon using elastography in a healthy population.^[2] We used R version 3.1.2 (“ICC.Sample.Size” packages) for analysis. To achieve an ICC of 0.85 in an observational study with two examiners, assuming a 2-tailed significance level of alpha 0.05 and a power of 80%, we estimated that 26 subjects were needed. After confirming the normal distribution of data using the Kolmogorov–Smirnov test, repeated measures analysis of variance was used to identify significant differences in the SWV values of MN, FDS, FDP, and TCL, and the MN CSA between motion combination (A) and the other five motions. In the case of a significant difference, the ad-hoc Tukey and Games-Howell tests were used to test pairwise differences among the six motions. The differences among SWV values from the six motions were compared using repeated measures analysis of variance. The ICC was calculated to examine the consistency between ARFI analysis by the two examiners; ICC values between 0.8 and 1 were defined as very reproducible, between 0.6 and 0.8 as moderately reproducible, and under 0.6 as not very reproducible.^[2] All statistical analysis was performed using SPSS version 19 (SPSS Inc. Chicago, IL) and tests were considered significant if the *P*-value was below 0.05.

3. Results

3.1. Patient characteristics

A total of 26 participants were initially screened, and none were excluded. Of the 26, 20 were male (76.9%) and six were female (23.1%). The mean age was 24.7 years (range 19–38 years, standard deviation [SD] was 3.7 years), mean height was 171.7 cm (range 157–185 cm, SD 6.6 cm), and mean weight was 69 kg (range 47–90 kg, SD 11.8 kg). One participant (3.8%) had a history of atopic dermatitis and asthma, all other participants had no comorbidities. Twenty-five participants were right-handed and one participant was left-handed.

3.2. Comparison of stiffness of the carpal tunnel structures and median nerve cross-sectional area among the motions

The mean SWV values of the structures of interest in the different motions and their interrelationships are shown in Table 1 and Figure 3. The MN, FDS, FDP, and TCL all showed significant differences in SWV in all six motions ($P < .001$). The SWV

Table 1
Ultrasonographic and acoustic radiation force impulse parameters of the carpal tunnel structures in the six wrist/finger motion combinations.

	(A) Wrist _{neu} , Finger _{neu}	(B) Wrist _{neu} , Finger _{grasp}	(C) Wrist _{neu} , Finger _{ext}	(D) Wrist _{ext} , Finger _{neu}	(E) Wrist _{ext} , Finger _{grasp}	(F) Wrist _{ext} , Finger _{ext}	
SWV (m/s)							
MN	2.3 (0.5)	2.7 (0.5)*	2.7 (0.4)*	2.9 (0.5)*	3.0 (0.5)*	3.1 (0.5)*	<.001
FDS	2.9 (0.2)	3.1 (0.4)*	3.2 (0.4)*	3.3 (0.4)*	3.4 (0.6)*	3.4 (0.4)*	<.001
FDP	3.2 (0.3)	3.7 (0.5)*	3.7 (0.5)*	3.7 (0.4)*	4.0 (0.9)*	3.7 (0.4)*	<.001
TCL	3.3 (0.4)	3.8 (0.5)*	3.7 (0.4)	3.8 (0.4)*	4.0 (0.6)*	4.1 (0.5)*	<.001
MN CSA (mm ²)	8.4 (1.5)	7.7 (1.5)	8.5 (1.6)	8.3 (1.8)	8.1 (1.5)	8.2 (1.5)	.527*

Data are presented as mean (standard deviation). The P-value was calculated using one-way analysis of variance.

FDP=flexor digitorum profundus, FDS=flexor digitorum superficialis, MN CSA=median nerve cross section area, MN=median nerve, SWV=shear wave velocity, TCL=transverse carpal ligament.

* P-value < .05 compared with (A) Wrist_{neu}, Finger_{neu}.

showed an increasing trend from (A) to (F) in all four structures. Post hoc analysis was performed between two motions. The intracarpal tunnel portion of the MN, FDS, and FDP showed significantly lower SWVs in motion (A) than in the other five motions. There were no statistical differences among motion (B) to (F) in all 3 structures. In the TCL, the SWV of motions (B), (D), (E), and (F) were significantly higher than that of motion (A). There were no significant differences between motion (A) and (C) or among motion (B), (C), (D), (E), and (F) in terms of SWV. The MN CSA showed no statistically significant differences among all motions (P = .527).

3.3. Intra-observer reliability

The conformity of the values measured by the two examiners using B-mode imaging and ARFI elastography is shown in Table 2. The intra-observer reliability for the MN SWV was 0.758 (P < .001), which values for the FDP, FDS, and TCL were

0.527, 0.506, and 0.522 (P < .001), respectively. The intra-observer reliability for the MN CSA was 0.344 (P = .005).

4. Discussion

In this study, the stiffness of intra-CT structures including the MN, FDS, FDP, and TCL was investigated by measuring the SWV in healthy volunteers in various wrist/finger motion combinations and comparing them with each other. The lowest stiffness was observed for all four structures of interest when a neutral position of the wrist and fingers was adopted.

Several studies have investigated the physiological mechanisms of structures in the CT during hand motion using magnetic resonance imaging,^[13–16] ultrasonography,^[17–20] direct CT pressure analysis,^[3,4,12,21] and cadaver studies.^[22,23] Elastography is a recently developed method for CT-structure evaluation.^[24–26] Elevated MN stiffness has been identified as a characteristic of CTS,^[27,28] and a system for the diagnosis of CTS as well as a grading system have been proposed.^[10,29] With regards to methodologies, ARFI elastography has the advantage that the Young’s modulus provides more precise calculations than strain elastography, therefore enabling a more quantitative and reproducible analysis.^[1]

The SWV value measured for MN in our study was 2.3 ± 0.5 m/s (mean ± SD) during motion (A), which is similar to the value of 2.97 ± 0.41 m/s (range: 2.21–3.80) reported by Arslan et al.^[1] The SWV of the flexor tendons in CT is, as yet, unreported.

Our data show that intra-CT structures such as the MN and flexor tendons are under considerably increased stress during wrist and finger motions compared with a neutral position. This can be attributed to the intra-CT pressure elevation and flexor-tendon displacement that occur during hand motion. Bower et al

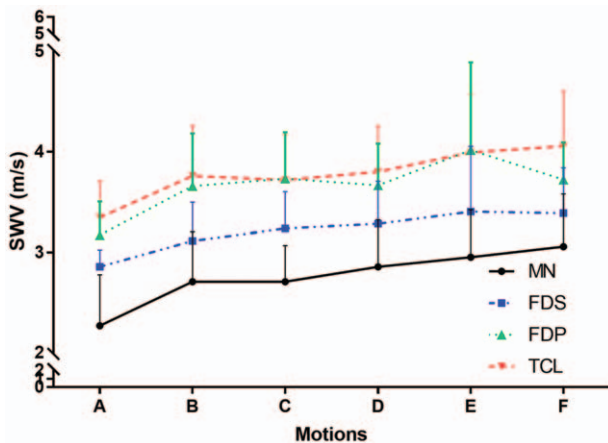


Figure 3. Measured shear wave velocities of carpal tunnel structures in different wrist/finger motion combinations. The median nerve, flexor digitorum superficialis, and flexor digitorum profundus showed significantly higher shear wave velocities in positions (B) to (F) than (A), while the transverse carpal ligament showed a significantly higher shear wave velocity in positions (B), (D), (E), and (F) compared with (A). The measured shear wave velocities of all target structures increased from (A) to (F), although the median nerve cross-sectional area was not significantly different between the wrist/finger motions. Bars indicate standard deviation. FDP=flexor digitorum profundus, FDS=flexor digitorum superficialis, MN=median nerve, SWV=shear wave velocity, TCL=transverse carpal ligament.

Table 2
Intraclass correlation coefficient of the acoustic radiation force impulse values of carpal tunnel structures.

	ICC	95% CI	P
MN	0.758	0.667–0.823	<.001
FDS	0.527	0.351–0.655	<.001
FDP	0.506	0.322–0.640	<.001
TCL	0.522	0.345–0.652	<.001
MN CSA	0.344	0.100–0.522	.005

CI=confidence interval, FDP=flexor digitorum profundus, FDS=flexor digitorum superficialis, ICC=intraclass correlation coefficient, MN=median nerve, MN CSA=median nerve cross section area, TCL=transverse carpal ligament.

reported that a narrowing of the CT area (CTA) and decreasing of the ratio of CT contents area (CTC_A) and CTA (CTC_A/CTA) occurred when the wrist was at 30° extension compared with a neutral or 30°-flexion position.^[15] Several studies have found that intra-CT pressure increases by up to 10 times during wrist extension compared with a neutral position.^[4,21] During wrist and finger motion, the MN moves to avoid compression by tendons or remains in situ to be compressed between the flexor tendons.^[6,7] The three factors of CTA narrowing, CT pressure elevation, and tendon displacement contribute to MN compression during wrist and finger motions.

Stiffness of the flexor tendons and TCL increase during wrist/finger motion. This can be attributed to two factors: direct compression and stretch of the structures. The flexor tendons and TCL are directly compressed during hand motions for the same reasons as the MN. Shen et al reported the SWV of the TCL to be 5.21 ± 1.08 m/s, which was greater than our result of 3.3 ± 0.4 , and the authors showed that the SWV was increased during compression compared to motions without compression.^[18] There have been reports of the SWV of the Achilles' tendon, which show similar results of increased SWV during ankle plantar flexion compared with a neutral position; in other words, an increase when the tendon is stretched.^[30,31] However, the SWV value of the FDP decreased in motions (C), (D), and (F) rather than consistently increasing from motion (B) through (F) as was observed for the MN, FDS, and TCL. Although this difference was not statistically significant, this indicates structural differences in the FDP compared with other structures. Further research is required to ascertain whether this was due to technical error, or whether this structure has intrinsically different characteristics as the center-most structure within the CT.

The SWV of the MN CSA did not show significant differences among all motions, but decreased as the position shifted from finger extension to flexion when the wrist was neutral, in line with the study of van Doesburg et al.^[5]

The inter-observer reproducibility was low compared to previous studies, especially those conducted on tendons.^[1,10] Low inter-observer correlation in SWV measurements of tendons has been reported by Aubry et al, who emphasized the need to consider two biases on future studies on the topic of tendon elasticity. One is bias due to the contraction of muscle being examined, and the other is bias due to the location and direction of the transducer and the positioning of the region of interest given the highly anisotropic characteristic of tendons.^[31]

This study has some limitations which should be acknowledged. First, the mean age of the participants was 24.7 (range 19–38) years, and there was a male dominance in the study population, which makes it difficult to generalize the results to all age and gender groups. Second, the SWV and MN CSA were not measured in positions of wrist flexion; further studies that include this position are needed. Third, the reproducibility of the MN CSA was low. This could have been due to difficulties in controlling the exact angle and position of the transducer on the various structures with each motion.^[31] Fourth, the 2×2 mm²-sized region-of-interest box that was used for measuring SWV could be smaller or larger than CSA of the structure of interest, which would result in bias.^[18]

In conclusion, this study demonstrates that the stiffness of intra-CT structures is greater during wrist and finger movements than when the wrist and fingers are in neutral positions, which provides insight into the pathophysiology of CTS. We also show that ARFI elastography can be used to differentiate delicate

changes in the stiffness of soft tissue. Therefore, ARFI elastography may enable diagnosis and determination of the grade of CTS and other entrapment neuropathies of the peripheral nerves.

Acknowledgments

We would like to offer special thanks to Suyeon Park, MS, biostatistician, for helping with statistical design and analysis. We also thank Mun Hwan Lee, Orthotist, the Jeonglib O & S.

Author contributions

Conceptualization: Sungche Lee, Eunsun Oh, Ji Woong Park.

Data curation: Sungche Lee, Jinmyong Kwak, Sanghoon Lee, Hyuncheol Cho.

Formal analysis: Sungche Lee, Jinmyong Kwak.

Funding acquisition: Ji Woong Park.

Investigation: Sungche Lee, Jinmyong Kwak, Hyuncheol Cho.

Methodology: Sungche Lee, Sanghoon Lee.

Project administration: Ji Woong Park.

Resources: Sanghoon Lee, Hyuncheol Cho.

Supervision: Eunsun Oh, Ji Woong Park.

Validation: Sungche Lee, Jinmyong Kwak.

Visualization: Sanghoon Lee, Eunsun Oh.

Writing – original draft: Sungche Lee.

Writing – review & editing: Eunsun Oh, Ji Woong Park.

Ji Woong Park: 0000-0001-7987-3581.

Ji Woong Park orcid: 0000-0001-7987-3581.

References

- Arslan H, Yavuz A, Ilgen F, et al. The efficiency of acoustic radiation force impulse (ARFI) elastography in the diagnosis and staging of carpal tunnel syndrome. *J Med Ultrason* 2001;2018;45:453–9.
- Fu S, Cui L, He X, et al. Elastic characteristics of the normal Achilles tendon assessed by virtual touch imaging quantification shear wave elastography. *J Ultrasound Med* 2016;35:1881–7.
- Werner CO, Elmqvist D, Ohlin P. Pressure and nerve lesion in the carpal tunnel. *Acta Orthop Scand* 1983;54:312–6.
- Werner R, Armstrong TJ, Bir C, et al. Intracarpal canal pressures: the role of finger, hand, wrist and forearm position. *Clin Biomech (Bristol, Avon)* 1997;12:44–51.
- van Doesburg MH, Henderson J, Yoshii Y, et al. Median nerve deformation in differential finger motions: ultrasonographic comparison of carpal tunnel syndrome patients and healthy controls. *J Orthop Res* 2012;30:643–8.
- Nakamichi K, Tachibana S. Transverse sliding of the median nerve beneath the flexor retinaculum. *J Hand Surg Br* 1992;17:213–6.
- Wang Y, Zhao C, Passe SM, et al. Transverse ultrasound assessment of median nerve deformation and displacement in the human carpal tunnel during wrist movements. *Ultrasound Med Biol* 2014;40:53–61.
- Wright TW, Glowczewskie F, Wheeler D, et al. Excursion and strain of the median nerve. *J Bone Joint Surg Am* 1996;78:1897–903.
- Wong SM, Griffith JF, Hui AC, et al. Carpal tunnel syndrome: diagnostic usefulness of sonography. *Radiology* 2004;232:93–9.
- Kantarci F, Ustabasioglu FE, Delil S, et al. Median nerve stiffness measurement by shear wave elastography: a potential sonographic method in the diagnosis of carpal tunnel syndrome. *Eur Radiol* 2014;24:434–40.
- Tatar IG, Kurt A, Yavasoglu NG, et al. Carpal tunnel syndrome: elastosonographic strain ratio and cross-sectional area evaluation for the diagnosis and disease severity. *Med Ultrason* 2016;18:305–11.
- Keir PJ, Bach JM, Rempel D. Effects of computer mouse design and task on carpal tunnel pressure. *Ergonomics* 1999;42:1350–60.
- Allmann KH, Horch R, Uhl M, et al. MR imaging of the carpal tunnel. *Eur J Radiol* 1997;25:141–5.
- Monagle K, Dai G, Chu A, et al. Quantitative MR imaging of carpal tunnel syndrome. *AJR Am J Roentgenol* 1999;172:1581–6.

- [15] Bower JA, Stanisz GJ, Keir PJ, et al. An MRI evaluation of carpal tunnel dimensions in healthy wrists: Implications for carpal tunnel syndrome. *Clin Biomech (Bristol, Avon)* 2006;21:816–25.
- [16] Keberle M, Jenett M, Kenn W, et al. Technical advances in ultrasound and MR imaging of carpal tunnel syndrome. *Eur Radiol* 2000;10:1043–50.
- [17] Wang Y, Filius A, Zhao C, et al. Altered median nerve deformation and transverse displacement during wrist movement in patients with carpal tunnel syndrome. *Acad Radiol* 2014;21:472–80.
- [18] Shen ZL, Vince DG, Li ZM. In vivo study of transverse carpal ligament stiffness using acoustic radiation force impulse (ARFI) imaging. *PLoS One* 2013;8:e68569.
- [19] Erel E, Dilley A, Greening J, et al. Longitudinal sliding of the median nerve in patients with carpal tunnel syndrome. *J Hand Surg Br* 2003;28:439–43.
- [20] Park D. Ultrasonography of the transverse movement and deformation of the median nerve and its relationships with electrophysiological severity in the early stages of carpal tunnel syndrome. *PM R* 2017;9:1085–94.
- [21] Rempel D, Keir P, Bach J. The dose±response relationship of wrist posture and carpal tunnel pressure. *Proceedings of the 43rd Annual Meeting, Orthopaedic Research Society* 1997:9-13.
- [22] Yoshii Y, Zhao C, Zhao KD, et al. The effect of wrist position on the relative motion of tendon, nerve, and subsynovial connective tissue within the carpal tunnel in a human cadaver model. *J Orthop Res* 2008;26:1153–8.
- [23] Zhao C, Ettema AM, Osamura N, et al. Gliding characteristics between flexor tendons and surrounding tissues in the carpal tunnel: a biomechanical cadaver study. *J Orthop Res* 2007;25:185–90.
- [24] Arda K, Ciledag N, Aktas E, et al. Quantitative assessment of normal soft-tissue elasticity using shear-wave ultrasound elastography. *AJR Am J Roentgenol* 2011;197:532–6.
- [25] Dirrichs T, Quack V, Gatz M, et al. Shear wave elastography (SWE) for the evaluation of patients with tendinopathies. *Acad Radiol* 2016;23:1204–13.
- [26] Ryu J, Jeong WK. Current status of musculoskeletal application of shear wave elastography. *Ultrasonography* 2017;36:185–97.
- [27] Wang Y, Qiang B, Zhang X, et al. A non-invasive technique for estimating carpal tunnel pressure by measuring shear wave speed in tendon: a feasibility study. *J Biomech* 2012;45:2927–30.
- [28] Orman G, Ozben S, Huseyinoglu N, et al. Ultrasound elastographic evaluation in the diagnosis of carpal tunnel syndrome: initial findings. *Ultrasound Med Biol* 2013;39:1184–9.
- [29] Miyamoto H, Halpern EJ, Kastlunger M, et al. Carpal tunnel syndrome: diagnosis by means of median nerve elasticity—improved diagnostic accuracy of US with sonoelastography. *Radiology* 2014;270:481–6.
- [30] Aubry S, Nueffer JP, Tanter M, et al. Viscoelasticity in Achilles tendonopathy: quantitative assessment by using real-time shear-wave elastography. *Radiology* 2015;274:821–9.
- [31] Aubry S, Risson JR, Kastler A, et al. Biomechanical properties of the calcaneal tendon in vivo assessed by transient shear wave elastography. *Skeletal Radiol* 2013;42:1143–50.